ISSN 1027-5495. Functional Materials, 28, No.2 (2021), p. 259-265.
doi:https://doi.org/10.15407/fm28.02.259

Dielectric tensor circular anisotropy in Co- and Fe-based ferromagnetic alloys

V.Kudin, S.Rozouvan, V.Staschuk

T.Shevchenko National University of Kyiv,
64/13 Volodymyrs'ka Str., 01601 Kyiv, Ukraine

Received November 12, 2020

It has been shown that the off-diagonal components of the dielectric tensor are interconnected by an additional relation, which is a consequence of the spatial isotropy of metal alloys. Anisotropy of the reflected circularly polarized light is possible in ferromagnetic alloys due to the magneto-optical Kerr effect which depends on the non-diagonal components. Spectral ellipsometric measurements in Co- and Fe-based alloys revealed this effect, which occurs when the direction of magnetization deviates from the normal to the sample surface. *Ab initio* electronic structure calculations for supercells with structures similar to the experimentally investigated alloys made it possible to construct dispersion curves of the dielectric tensor components and to confirm the experimental results.
Keywords: ferromagnetic alloys, magneto-optical Kerr effect, circular anisotropy.

Кругова анізотропія тензора діелектричної проникності у феромагнітних сплавах на основі Co і Fe. *В.Кудін, С.Розуван, В.Стащук*

Показано, що недіагональні компоненти тензора діелектричної проникності металевих сплавів пов'язані додатковим співвідношенням, яке є наслідком просторової ізотропності середовища. При магнітооптичному ефекті Кера у феромагнітних сплавах, який залежить від недіагональних компонент можлива анізотропія відбитого циркулярно поляризованого світла. Спектрально-еліпсометричні вимірювання в сплавах на основі Co–Fe виявили даний ефект, що виникає при відхиленні напрямку намагніченості від нормалі до поверхні зразка. Квантовомеханічні розрахунки електронної структури для надкомірок зі складом аналогічним до експериментально досліджених сплавів дозволили побудувати дисперсійні криві компонент тензора діелектричної проникності і підтвердити експериментальні результати.

Показано, что недиагональные компоненты тензора диэлектрической проницаемости металлических сплавов связаны дополнительным соотношением, которое является следствием пространственной изотропности среды. При магнитооптическом эффекте Кера в ферромагнитных сплавах, который зависит от недиагональных компонент, возможна анизотропия отраженного циркулярно поляризованного света. Спектральноелипсометрични измерения в сплавах на основе Co–Fe обнаружили данный эффект, возникающий при отклонении направления намагниченности от нормали к поверхности образца. Квантовомеханические расчеты электронной структуры для суперячеек с составом аналогичным экспериментально исследуемым сплавам, позволили построить дисперсионные кривые компонент тензора диэлектрической проницаемости и подтвердить экспериментальные результаты.

1. Introduction

The magneto-optical Kerr effect (MOK) has been actively studied in recent decades in a wide class of ferromagnetic materials. The availability of commercially suitable ellipsometers made it possible to measure ellipsometric parameters Δ and ψ with an accuracy of hundredths of a degree; this al-

lowed experimental studying the components of the dispersion curves of the dielectric tensor, which are also responsible for the Kerr effect. The study of the spectral behavior of off-diagonal components of the dielectric constant ε, which are responsible for the rotation of the plane of polarization of linearly polarized light reflected from the surface, allows us to investigate the densities of electronic states of these compounds. From this point of view, alloys based on d-metals attract attention due to their distinctive magneto-optical properties associated with their electronic structure and off-diagonal elements of the dielectric tensor.

In recent decades, due to the development of technology, it has become possible to obtain structures (materials) with fundamentally different properties compared to well-known materials. One of examples is related to two-phase systems: metal ferromagnetic granules surrounded by a dielectric matrix (core/shell structure) [1]. These include, in particular, compounds $(Fe_{40}Co_{40}B_{20})_x$–$(SiO_2)_{100-x}$ consisting of two amorphous phases. This type of systems is interesting both from a theoretical and practical point of view, since they have a number of remarkable properties [2]; in particular, this concerns the magnetization process [3], Hall effect [4], high dielectric losses in the RF range [5], boron content influence on coercivity and anisotropy [6]. It was found that the observed effect of magnetic anisotropy in such compounds is associated with the complex magnetic structure of the FeCo and FeCo–SiO_2 layers [7]. Recent studies applying atomic spatial resolution scanning tunneling microscopy revealed a complicated morphology of $(Fe_{40}Co_{40}B_{20})_x$–$(SiO_2)_{100-x}$ substances [8]. Such systems are promising to design numerous devices and elements of electronics; perhaps, first of all, we should mention the elements used as magnetic heads for recording and reading information, which are characterized, in comparison with the existing ones, by low energy losses due to eddy currents (Foucault currents) and, naturally, a significant reduction in electrical noise.

The theoretical formalism connecting the tensor elements with ellipsometric experimental parameters Δ and ψ has been developed in detail; an exception is the cases when the tensor components are a function of the orientation of the spontaneous magnetization in the sample. Within the framework of Kerr's targeted optical studies with a wide class of compounds based on Co and Fe, it is also important to carry out a theoretical analysis of spectral-ellipsometric measurements; for example, perform *ab initio* calculations of the electronic structure to analyze the experimental dispersion curves using the quantum mechanical approach.

Optical techniques, in our opinion, are the most informative of a number of the most frequently used experimental methods for obtaining direct information on the spectra of electronic states of the objects under study in a wide range of energies. In the simplest cases, it corresponds to the band gap $h\nu = 1–5$ eV, which seems to be the most significant energy interval for practical applications. Thus, spectral ellipsometric experiments are the most informative for such tasks; particularly, in the case of ferromagnetic samples, it is possible to separate the role of electrons with different spins. A comprehensive study of the electronic properties of such complex compounds as $(Fe_{40}Co_{40}B_{20})_x$–$(SiO_2)_{100-x}$ should include the use of a set of experimental and theoretical studies of both optical and magneto-optical properties in a wide range of the spectrum.

The aim of this work was to obtain information about all components of the dielectric tensor and compare them with the theoretically calculated data (in the framework of quantum mechanical theory) and, ultimately, to obtain information about the electronic structure of studied ferromagnetic samples. As the objects of study, the compounds $(Fe_{40}Co_{40}B_{20})_x$–$(SiO_2)_{100-x}$ were selected, the optical and magneto-optical properties of which were studied in a wide range of the spectrum $h\nu$ =1.24–5.15 eV.

2. Theory: dielectric permeability tensor of optically active isotropic medium

From the classical optics, the interaction of light with a spatially isotropic substance, which leads to the rotation of the polarization plane of linearly polarized light due to magneto-optical effects, is described by an antisymmetric dielectric tensor [9]:

$$\begin{vmatrix} \varepsilon_{xx} & -\varepsilon_{xy} & 0 \\ \varepsilon_{xy} & \varepsilon_{yy} & 0 \\ 0 & 0 & \varepsilon_{zz} \end{vmatrix} = \begin{vmatrix} \varepsilon_{xx} & -\varepsilon_{xy} & 0 \\ \varepsilon_{xy} & \varepsilon_{xx} & 0 \\ 0 & 0 & \varepsilon_{zz} \end{vmatrix}. \quad (1)$$

For light in an isotropic medium, the diagonal elements of the dielectric tensor

$|\varepsilon_{xx(yy)} \pm \varepsilon_{xy(yx)}| = |\varepsilon_{zz}|$ are the same, since there is no optical birefringence with the optical axis (axes). Equation (1) is also valid for an isotropic ferromagnet with magnetization along *OZ* axis, in which there is the magneto-optical Kerr effect, and the values of the off-diagonal elements are usually orders of magnitude smaller than the diagonal elements of the tensor; and they are responsible for rotating the polarization plane. Performing the eigendecomposition of matrix from Eq. (1) we can obtain:

$$\begin{vmatrix} \varepsilon_{xx}+i\varepsilon_{xy} & 0 & 0 \\ 0 & \varepsilon_{xx}-i\varepsilon_{xy} & 0 \\ 0 & 0 & \varepsilon_{zz} \end{vmatrix}. \quad (2)$$

Here, the values of the diagonal elements of the matrix are λ solutions of the spectral problem for the matrix ε: $\varepsilon V - \lambda V = 0$ (V is eigenvector). From a physical point of view, diagonal elements should be interpreted as three equatorial axes of the triaxial ellipsoid of dielectric constants, and their values must satisfy the condition of spatial isotropy of the medium, which in the case of Eq. (2) obviously takes place:

$$|\varepsilon_{xx} + i\varepsilon_{xy}| = |\varepsilon_{xx} - i\varepsilon_{xy}|. \quad (3)$$

Let us consider now a more complex case, which is actually always registered in experiments, when the components of the dielectric tensor are complex numbers:

$$\begin{vmatrix} \varepsilon^{(1)}_{xx}+i\varepsilon^{(2)}_{xx} & -\varepsilon^{(1)}_{xy}-i\varepsilon^{(2)}_{xy} & 0 \\ \varepsilon^{(1)}_{xy}+i\varepsilon^{(2)}_{xy} & \varepsilon^{(1)}_{xx}+i\varepsilon^{(2)}_{xx} & 0 \\ 0 & 0 & \varepsilon_{zz} \end{vmatrix}, \quad (4)$$

where the superscripts (1) and (2) denote, respectively, the real and imaginary components of the dielectric tensor. After the eigendecomposition of the matrix from Eq. (4) we obtain:

$$\varepsilon = \begin{vmatrix} \varepsilon^{(1)}_{xx}+\varepsilon^{(2)}_{xy} + i\varepsilon^{(2)}_{xx} + i\varepsilon^{(1)}_{xy} & 0 & 0 \\ 0 & \varepsilon^{(1)}_{xx}-\varepsilon^{(2)}_{xy}+i\varepsilon^{(2)}_{xx}-i\varepsilon^{(1)}_{xy} & 0 \\ 0 & 0 & \varepsilon_{zz} \end{vmatrix}. \quad (5)$$

For a spatially isotropic medium, the first two diagonal complex components of Eq. (5) must have the same absolute values, which results in the following relation:

$$\mathrm{Re}(\varepsilon_{xx})\mathrm{Im}(\varepsilon_{xy}) - \mathrm{Im}(\varepsilon_{xx})\mathrm{Re}(\varepsilon_{xy}) = 0. \quad (6)$$

As we can see, the isotropic medium symmetry leads to an additional relation between the off-diagonal components of the dielectric tensor. Practically, the dielectric permeability tensor for ferromagnetic alloys is isotropic when linearly polarized light is reflected — the diagonal elements of the tensor are equal ($\varepsilon_{xx} = \varepsilon_{yy}$), since the alloys generally have a polycrystalline or amorphous structure. At the same time, anisotropy of circularly polarized light is possible, if the relation (6) is not satisfied when the magnetization vector is not perpendicular to the sample surface. In the case of linearly polarized light reflection having nonzero *p*- and *s*-components, the ellipticity of the reflected beam will depend on the angle of rotation of the sample around the normal to its surfaces due to the different tensor off-diagonal elements $\varepsilon_{yx} \neq \varepsilon_{xy}$ (see relation (3)).

From a purely practical point of view, Eq. (6) allows analyzing the experimental data for the agreement of the experimental data with the theoretical model of the magneto-optical Kerr effect with the magnetization perpendicular to the sample surface.

3. Results and discussion

Samples of composite structures $(Fe_{40}Co_{40}B_{20})_x$–$(SiO_2)_{100-x}$ with different contents of a magnetic phase (x = 19, 33, 41, 56 and 100 %) were obtained by ion-plasma deposition in an atmosphere of pure argon from two different targets; different distances from the target, deposition rates varying with the temperature of glass substrates, and heat treatment modes were used. As a result, it was possible to form structures with transverse dimensions of metal granules about 10 nm, which became slightly smaller as the content of the metal phase decreased. The thicknesses of the deposited films were about 1 μm. Spectral studies of all components of the dielectric tensor ε were carried out by measuring the ellipsometric parameters Ψ and Δ at different angles of incidence of light φ = 45°, 55°, 65° and 75° and magneto-optical angles of the Kerr effect in a wide spectral range $h\nu$ = 1.24–5.15 eV (λ = 0.24–1.0 μm) on a spectral ellipsometer Woollam M-2000.

The ellipsometric parameters were measured by the technique of reflective ellipsometry, since the studied samples strongly absorbed light in near ultraviolet, visible and near infrared spectral ranges. The method is based on the central ellipsometry equation:

$$\frac{r_p}{r_s} = \mathrm{tg}\psi \cdot e^{i\Delta}, \quad (7)$$

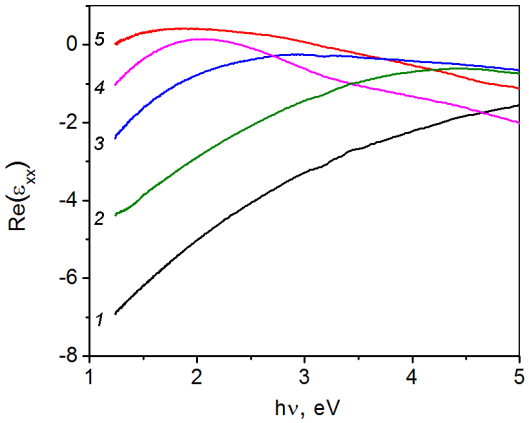

Fig. 1. Dielectric tensor diagonal elements $|\varepsilon_{xx}|$ in $(Co_{41}Fe_{39}B_{20})_x(SiO_2)_{100-x}$: *1)* $x = 100$; *2)* $x = 56$; *3)* $x = 41$; *4)* $x = 33$; *5)* $x = 19$.

where r_p, r_s are the complex amplitude reflection coefficients in the p- and s-planes, tgψ is the absolute value of the ratio of the amplitudes of the reflection coefficients in the p- and s-planes, Δ is the phase difference between the p- and s-components of the reflected wave electric vector.

Refractive indices n and absorption numbers k were calculated by known expressions from the experimental values of Ψ and Δ obtained on the ellipsometer in the spectral range $\lambda = 0.24–1$ μm in the model of a semi-infinite medium:

$$n = \sin\varphi\,\mathrm{tg}\varphi\,\frac{\cos 2\psi}{1 + \sin 2\psi\cos\Delta}, \qquad (8)$$

$$k = \sin\varphi\,\mathrm{tg}\varphi\,\frac{\sin 2\psi\sin\Delta}{1 + \sin 2\psi\cos\Delta},$$

where φ is the light incidence angle. The experimental accuracy of measuring the ellipsometric parameters Ψ and Δ, for the angle of incidence $\varphi = 75°$ (in the vicinity of the main angle), should be the highest. However, our experiments showed that the average deviation of the standard error of the processed experimental data did not exceed 3 % at all angles of incidence $\varphi = 45°$, 55°, 65° and 75° over the spectral range of measurements. The high accuracy of measurements is the result of a high precision of recording the intensities of light fluxes in modern ellipsometers, which makes it possible to register light signals of relatively low power when measuring small numbers of light ellipticity in the magneto-optical Kerr effect. Dielectric constants and anisotropy curves obtained from the experimental data are shown in Fig. 1–3.

The diagonal components of the dielectric tensor ε_{xx} were calculated from the experimental data. The absolute values of dispersion curves of the diagonal components of the dielectric tensor are shown in Fig. 1. As we can see, the curves monotonically increase their values with a decrease in the concentration of SiO_2 in the samples.

Applying the unified expression [10], off-diagonal components of the dielectric tensor were determined from the measured values of the complex Kerr angle $\theta_s + i\eta_s$ of the reflected light:

$$\theta + i\eta \approx \frac{i\varepsilon_{xy}}{(\varepsilon_{xx} - 1)\sqrt{\varepsilon_{xx}}}. \qquad (9)$$

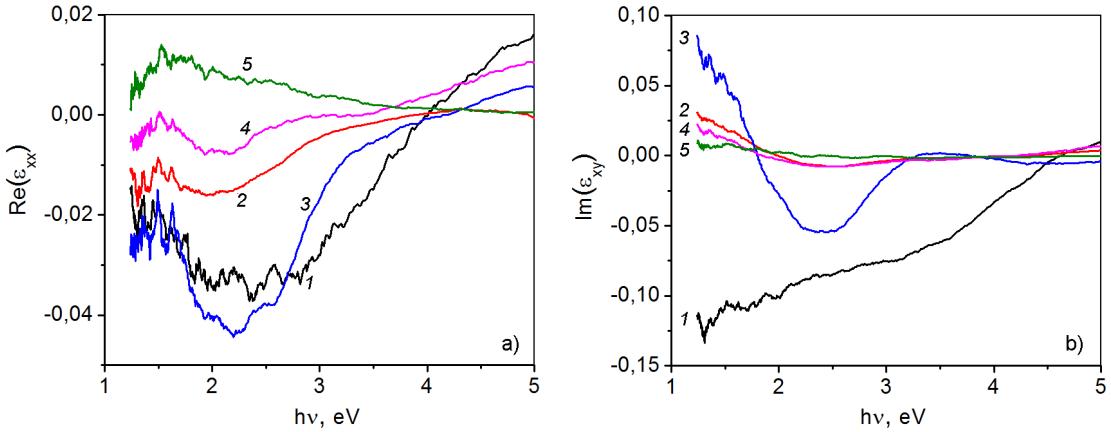

Fig. 2. Dielectric tensor off-diagonal elements $|\varepsilon_{xy}|$ in $(Co_{41}Fe_{39}B_{20})_x(SiO_2)_{100-x}$: *1)* $x = 19$; *2)* $x = 33$; *3)* $x = 41$; *4)* $x = 56$; *5)* $x = 100$.

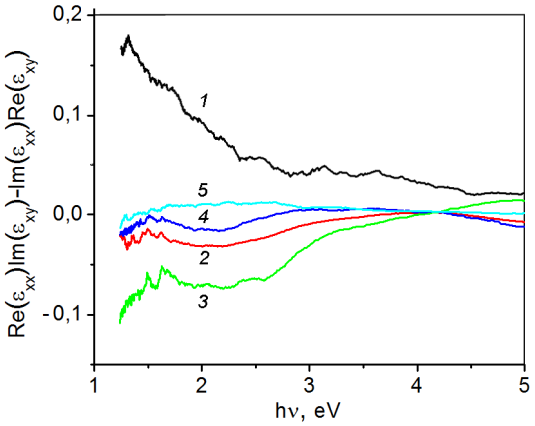

Fig. 3. Anisotropy of optical activity in $(Co_{41}Fe_{39}B_{20})_x(SiO_2)_{100-x}$: *1)* x=19; *2)* x=33; *3)* x=41; *4)* x=56; *5)* x=100.

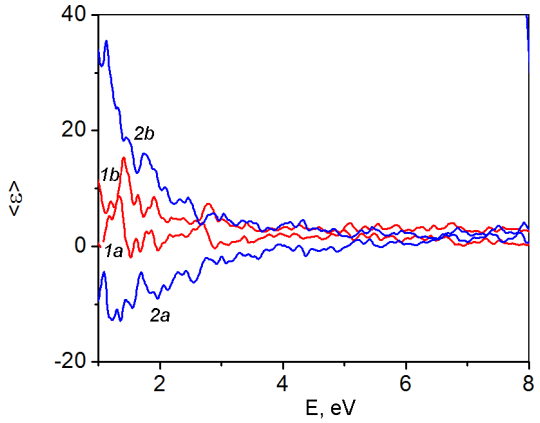

Fig. 4. Calculated direction-averaged real (a) and imaginary (b) components of the dielectric constant for supercells with *1)* 40% Fe, 40% Co, 17.5% B, 2.5% Si and *2)* 40% Fe, 40% Co, 20% B.

Complex MO Kerr angles are in fact the phase difference between the left and right circular polarized light reflected from the sample:

$$\theta_s + i\eta_s \approx r_{ps}/r_{ss}, \qquad (10)$$
$$-\theta_p + i\eta_p \approx r_{sp}/r_{pp}.$$

The r_{ij} coefficients are elements of the off-diagonal Jones matrix R ($r_{ps} = -r_{sp}$ and $r_{pp} = r_{ss}$) which describes reflection from an optically active media:

$$R = \begin{vmatrix} r_{pp} & r_{ps} \\ r_{sp} & r_{ss} \end{vmatrix}. \qquad (11)$$

Equation (10) is similar to expression (7), since it similarly connects the light amplitude and phase characteristics with the reflection coefficients of a sample. The difference between (7) and (10) expressions is that in the latter case, we have the light reflection from an optically active medium and operate with the parameters of circularly polarized light in contrast to *s*- and *p*-components in (7).

As we can see from Fig. 1, the diagonal component of the dielectric tensor changes monotonically at 2.2 eV with a change in the content of nonmetallic components in the sample. In Fig. 2 we also see changes in the anisotropy of circular polarization in the same spectral region, but these changes are already nonmonotonic due to the different orientations of magnetization in the ferromagnetic samples. For magnetization perpendicular to the sample surfaces (Fig. 3), the curves should be located near the abscissa axis. In fact, we do not control the direction of magnetization in the samples and therefore, in contrast to Fig. 1, the dependences of Fig. 2b change nonmonotonically as a function of the concentration of the nonmagnetic component (SiO_2).

If the magnetic induction vector is exactly perpendicular to the surface of the sample, we cannot register the anisotropy of the circular polarization of light due to the parity of all directions along the plane of the sample. This is almost true at concentrations x = 33, 56, 100 in Fig. 3. As can be seen from the plot there, the MO Kerr effect anisotropy in these cases is relatively insignificant. At concentrations x = 19, 41, the vectors of magnetic induction are inclined with respect to the normals to the surfaces forming specific directions on the samples surfaces.

We calculated optical properties of our samples by the method of all-electron full potential linearized augmented plane waves (LAPW) implemented in optics subroutines of the ABINIT software in the LINUX operating system [11]. The method was developed as a very robust and precise *ab initio* electronic structure technique having high efficiency to simulate the electronic properties of materials on the basis of density-functional theory. It allows solving the Kohn-Sham equations for the density of electronic states of the ground state and the parameters of the energy bands of a many-electron system by applying supercell partitioning and by introducing a combining basis set of LAPW's according to the linear variation method. The matrix elements of dipole transitions are estimated in detail in LAPW basis, taking into account the inter-

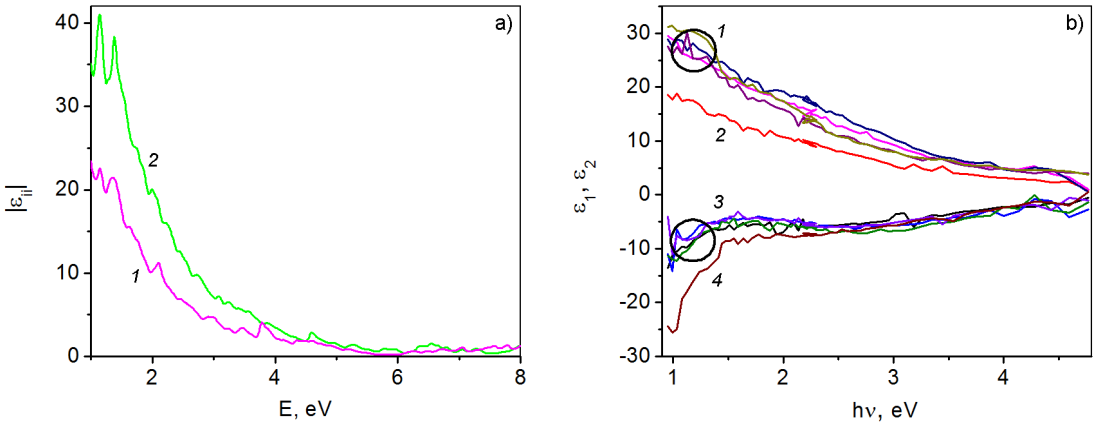

Fig. 5. a) Calculated absolute values of the dielectric constant for the supercell 40 % Fe, 40 % Co, 20 % B. *1)* ε_{xx} and ε_{yy} and components, *2)* ε_{zz} component, b) Measured real and imaginary parts of the dielectric constant for alloys Fe_xCo_{100-x}. *1)* imaginary part x = 10, 20, 40, 50 (marked with a circle), *2)* imaginary part x = 70, *3)* *real part* x = 20, 40, 50, 70 (marked with a circle), *4)* the real part x = 10.

band as well as intraband contributions to the dielectric tensor.

The first step of our calculation included the optimization of supercell parameters using norm-conserving pseudopotentials for Fe, Co and B atoms. We did a convergence test changing the kinetic energy cutoff which controls the number of plane waves at a point in the Brillouin zone. By increasing the energy, we achieved a relative accuracy of 0.1 % for the lattice parameters performing successive optimizations with different energies. A similar problem of calculation accuracy is associated with the discretization of the Brillouin zone to achieve a compromise between the requirements for the integration accuracy in the Brillouin zone and a smaller number of k-points. We mainly used the Monkhorst-Pack k-point grid with testing the k-point convergence. Using this grid takes time and computers with a lot of memory. In this case a computer with a 64-bit processor with ability to address random access memory above a 3 gigabytes barrier was required for the numbers of k points higher than in a 6×6×6 grid. The ABINIT optics subroutine which includes the computation of $\partial H/\partial k$ matrix elements (H is the Hamiltonian), required a few steps of calculations using the non-self-consistent field method additionally to the self-consistent field method and taking into account unoccupied states. Grid dimensions for our supercells were determined in order to achieve the specified accuracy of 0.1 % in the calculations of convergence. The presented calculations were performed with maximum grids of 16×16×16 k-points.

The results of the calculations are shown in Figs. 4, 5a. Two particular moments should be mentioned regarding the results. First, the values of the dielectric constant decrease with an increase in the content of silicon atoms (Fig. 4). From a qualitative physical point of view, this is absolutely logical — the density of electronic states in the conduction band decreases with a decrease in the concentration of metal atoms. It leads to a decrease in the number of electrons in the conducting band and to a decrease in the number of interband/intraband optical transitions. Second, supercells with asymmetrically located silicon atoms cause spatial anisotropy of the calculated dielectric constant (Fig. 5a). In polycrystalline samples, the individual cells with structures similar to that analyzed above are chaotically oriented, and the components of the dielectric tensor are averaged which leads to the degeneration of the tensor in to a scalar.

Results of spectral ellipsometric measurements of Fe-Co alloys with different concentrations are presented in Fig. 5b. We can see that the curve of the dielectric constant real part at low Co concentrations (x = 10) differs from others. This is consistent with the phase diagram of the Fe–Co alloy [12] at these concentrations with a two-phase region at room temperature. In fact, the course of the curve (*4*) in Fig. 5b confirms the results of the theoretical analysis, in which crystal lattice irregularities (in our case, clusters of two different crystal lattices) affect the dielectric constant of the

substance due to additional surface electronic states at the phase boundaries.

The difference in the shapes of the imaginary part of the dielectric constant for the $Fe_{70}Co_{30}$ alloy ($x = 70$) is a consequence of the electromagnetic wave attenuation due to the lesser influence of eddy currents (magnetic re-ordering in the Fe–Co phase diagram).

The abnormal course of the dielectric constant curves at Co–Fe concentrations of 9:1 can be explained as a violation of the periodic potential function of the crystal lattice due to the existence of several phases with different types of crystal structure. Violation of the condition of infinity of the crystal lattice leads to the appearance of additional states localized near the surfaces of granules of various crystalline phases. These additional surface states may be responsible for further increasing the real part of the dielectric constant. The integral of the energy density of states remains unchanged; in fact, the density of near-surface states increases due to the migration of some energy levels from the main energy zones of Co and Fe to the band gap. The sample surface affects the perturbations of the periodic potential function of the crystal lattice. Our experimental technique — spectral ellipsometry — allows you to effectively record the properties of the sample surfaces.

4. Conclusions

We can draw the following conclusions in accordance with the presented studies of Fe and Co based alloys which included theoretical analysis, first principles electronic structure calculations and spectral ellipsometric measurements.

The real and imaginary parts of the diagonal and off-diagonal components of the dielectric tensor of a polycrystalline ferromagnet with a magnetization vector orthogonal to its surface are linked by an additional relation derived for a spatially isotropic ferromagnetic material.

The experimental dispersive curves of the magneto-optical Kerr effect should be additionally examined applying the developed theoretical expression to check the magnetization direction in the samples. Analysis by registering only Kerr angles without determining the direction of magnetization leads to a systematic measurement error.

The dielectric tensor numbers of Fe–Co ferromagnetic alloys with inclusions of a non-magnetic phase are a function of the relative content of the magnetic phase in the samples. The effect is influenced by the reduction of density of electronic states in the conduction band which affects the dielectric permittivity numbers of the media. The calculations of the electronic structure of the supercells, similar to the experimentally studied samples confirmed these experimental results.

The values of the elements of the dielectric tensor in the ferromagnetic Fe–Co alloys demonstrate its relative equivalence at different contents of Fe and Co, except for the cases of the presence of two phases in the alloy with different crystal lattice ordering. The formation of the two types of clusters with different crystalline lattices results in the appearance of surface states in the energy band gap. The states are spatially localized at the boundaries of the clusters. The additional states result in a change in the spectral curves of the dielectric tensor at a Co concentration of about 10 %.

References

1. R.Tang, T.Li, Z.Wu et al., *IEEE Trans. Magnet.*, **47**, 3456 (2011).
2. F.F.Yang, S.S.Yan, M.X.Yu et al., *J. Appl. Phys.*, **111**, 113909 (2012).
3. J.Long, M.E.McHenry, D.E.Laughlin et al., *J. Appl. Phys.*, **103**, 07E710 (2008).
4. Y.O.Mikhailovsky, D.E.Mettus, A.P.Kazakov et al., *JETP Letters*, **97**, 473 (2013).
5. O.Dunets, Y.Kalinin, M.Kashirin, A.Sitnikov, *J. Techn. Phys.*, **58**, 1352 (2013).
6. K.Inyoung, K.Jongryoul, K.Ki Hyeon, M.Yamaguchi, *IEEE Trans. Magn.*, **40**, 2706 (2004).
7. L.Zhang, W.B.Zhu, H.Y.Zheng et al., *J. Appl. Phys.*, **117**, 17C110 (2015).
8. V.O.Lysiuk, S.G.Rozouvan, V.S.Staschuk, *J. Opt. Soc. Am. B*, **35**, 1628 (2018).
9. J.Hamrle, S.Blomeier, O.Gaier et al., *J. Phys. D: Appl. Phys.*, **40**, 1563 (2007).
10. V.Stashchuk, V.Stukalenko, S.Rozouvan, V.Lysiuk, *Ukr. J. Phys.*, **65**, 310 (2020).
11. C.Ambrosch-Draxl, J.O.Sofo, *Computer Phys. Commun.*, **175**, 1 (2006).
12. I.Ohnuma, H.Enoki, O.Ikeda et al,, *Acta Materialia*, **50**, 379 (2002).